FULL PAPER

Ab Initio Calculations of Vibrational Frequencies, Potential Functions of Internal Rotations and Vibrational Infrared and Raman Spectra for 3,3,3-Trifluoropropanal

Wolfgang Förner and Hassan M. Badawi

Department of Chemistry, King Fahd University of Petroleum and Minerals, Dhahran 31261, Saudi Arabia.
E-mail: hbadawi@kfupm.edu.sa

Abstract The conformational behavior and structure of 3,3,3,-trifluoropropal have been investigated by utilizing *ab initio* calculations with the 6-31G** basis set (valence double zeta basis with polarization functions on all atoms) at the restricted Hartree Fock (RHF), second-order Møller-Plesset perturbation (MP2), and Density Functional (B3LYP) levels. The molecule is predicted to have a *cis* ⇔ *gauche* conformational equilibrium. Full optimization of the transition states was performed and the rotational barriers of both the CHO and CF_3 rotors were calculated. Vibrational frequencies were computed at the three levels and the zero-point corrections were included into the calculated asymmetric CHO rotational barrier. Complete vibrational assignments were made on the basis of normal coordinate calculations for both stable conformers of the molecule.

Keywords Vibrational spectra and assignments, Rotational barriers, 3,3,3-trifluoropropanal

Introduction

The investigation of structural and conformational stability of many aldehydes and their halo-derivatives has attracted attention for many years [1-17]. The chemical reactivity of aldehydes in synthetic chemistry attracted our interest in order to study their vibrational and rotational spectra and to determine their conformational equilibrium. Several of these molecules were relatively large cyclic compounds or mol-

ecules with two rotors [14-17]. The increase of molecular size along with the increase in the number of substituent leads to very complex spectra. Hence, the spectral and conformational analysis of such molecular systems are always a challenge to spectroscopist. The interpretation of such molecular spectra is extremely difficult and sometimes even impossible, because there are more degrees of freedom than can be determined from experimental data. Therefore *ab initio* calculations were used as a reliable source of structural information that provides a powerful tool for spectroscopists [13-23].

Halopropanals and halopropionyl halides are of special structural interest [7,16,17]. In these compounds there are two internal rotors that control their conformational preference, the carbonyl and the halomethyl groups. The rotation

Correspondence to: H.M. Badawi

Dedicated to Professor Paul von Ragué Schleyer on the occasion of his 70th birthday

Table 1 *Structural parameters, total dipole moment, and rotational constants of 3,3,3-trifluoropropanal*

Parameter	HF/6-31G**		MP2/6-31G**		B3LYP/6-31G**		Microwave [a]	
	Cis	Gauche	Cis	Gauche	Cis	Gauche	Cis	Gauche
Bond lengths (Å)								
$r(C_1-C_2)$	1.508	1.505	1.506	1.503	1.516	1.513	1.504	1.509
$r(C_1-C_3)$	1.512	1.516	1.513	1.515	1.518	1.529	1.523	1.519
$r(C_3=O_4)$	1.184	1.185	1.220	1.221	1.207	1.208	1.210	1.210
$r(C_3-H_5)$	1.095	1.093	1.104	1.102	1.112	1.110	1.115	1.115
$r(C_2-F_6)$	1.327	1.320	1.356	1.349	1.355	1.347		
$r(C_2-F_7)$	1.318	1.324	1.348	1.353	1.345	1.350		
$r(C_2-F_8)$	1.318	1.326	1.348	1.356	1.345	1.354		
$r(C_1-H_9)$	1.086	1.082	1.091	1.087	1.097	1.092	1.105	1.105
$r(C_1-H_{10})$	1.086	1.086	1.091	1.092	1.097	1.097	1.105	1.105
Bond angles (deg)								
$(C_2C_1C_3)$	115.0	112.8	114.2	113.8	115.2	112.7	113.8	111.7
$(C_1C_3O_4)$	125.1	122.1	124.7	122.6	125.3	122.9	124.9	125.1
$(C_1C_3H_5)$	113.8	116.6	114.0	115.8	113.3	115.4	115.1	115.1
$(C_1C_2F_6)$	109.6	111.5	110.0	111.8	109.8	111.6		
$(C_1C_2F_7)$	112.1	111.4	111.8	111.0	111.9	111.3		
$(C_1C_2F_8)$	112.1	111.3	111.8	111.0	111.9	111.1		
$(C_2C_1H_9)$	108.4	109.6	108.5	109.7	108.7	110.0	107.2	107.2
$(C_2C_1H_{10})$	108.4	107.7	108.5	107.6	108.7	107.5	107.2	107.2
$(F_6C_2C_1C_3)$	180.0	180.8	180.0	181.1	180.0	179.2		
$(O_4C_3C_1C_2)$	0.0	149.2	0.0	139.5	0.0	141.7	0.0	128.3
$(F_7C_2C_1F_6)$	119.2	120.4	119.2	120.5	119.2	120.5		
$(F_8C_2C_1F_6)$	-119.2	-120.1	-119.2	-120.3	-119.2	-120.1		
$(H_9C_1C_2C_3)$	122.1	122.0	122.1	121.5	122.3	122.5		
$(H_{10}C_1C_2C_3)$	-122.1	-120.1	-122.1	-120.1	-122.3	-119.6		
Dipole moment (Debye)								
μ_t	4.0	1.5	4.3	1.9	3.5	1.5		
Rotational Constants (MHz)								
A	4864	5335	4702	5114	4707	5122		
B	2015	1623	1999	1620	1967	1600		
C	1907	1606	1896	1604	1865	1585		

[a] Data are obtained for propanal [28]

of these two rotors around C-C bonds results in a complex conformational equilibrium. Therefore, the energy optimization and the calculation of the asymmetric potential function in such molecular systems will be useful to spectroscopists. In the present study we have carried out an investigation of the internal rotations and calculated the vibrational frequencies for 3,3,3-trifluoropropanal. Also, the vibrational infrared and Raman spectra of the molecules were calculated. The zero-point correction was included to the rotational barriers of the molecules. We have used a valence double zeta basis set with polarization functions on all atoms, which should be of sufficient flexibility for our purpose (a minimal or simple double zeta basis set would of course be insufficient). This is true especially because there are only

first and second row atoms in our molecular system. The results of this work are presented herein.

Ab initio calculations

The GAUSSIAN 94 program [24] running on an IBM RS/6000 model 7015-R24 workstations, was used to carry out the LCAO-MO-SCF Restricted Hartree Fock calculations. The 6-31G** basis set was used to optimize the structures and predict the energies and dipole moments of 3,3,3-trifluoropropanal in its stable conformations. The calculations were extended to the second-order Møller-Plesset perturbation MP2 [25] and density functional B3LYP [26,27]

Table 2 *Computed total energies and zero-point corrections (hartrees) and rotational barriers (kcal·mol⁻¹) in 3,3,3-trifluoropropanal [a]*
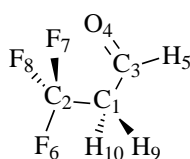
	HF/6-31G**	MP2/6-31G**	B3LYP/6-31G**
Total energies:			
Cis	-488.53953	-489.62095	-490.86559
Gauche	-488.54084	-489.62192	-490.86700
TS	-488.53714	-489.61909	-490.86363
Cis-Gauche barrier	1.500	1.167	1.230
Gauche-Cis barrier	2.322	1.776	2.115
Sum of total and zero point energies:			
Cis	-488.47237	-489.55768	-490.80386
Gauche	-488.47374	-489.55865	-490.80522
TS	-488.47007	-489.55593	-490.80196
Zero point correction:			
Cis	0.06717	0.06327	0.06173
Gauche	0.06710	0.06328	0.06178
TS	0.06707	0.06315	0.06167
Corrected cis-gauche barrier	1.443	1.098	1.192
Corrected gauche-cis barrier	2.303	1.707	2.046

[a] TS denotes the transition state

Table 3 *Calculated potential constants (kcal·mol⁻¹) for the internal rotation of CHO and CF₃ rotors in 3,3,3-trifluoropropanal*

Potential constants	HF/6-31G**	MP2/6-31G**	B3LYP/6-31G**
CHO rotor			
V_1	-1.64	-1.19	-1.46
V_2	1.41	0.77	1.12
V_3	1.31	1.21	1.25
V_4	0.37	0.25	0.27
V_5	0.39	0.42	0.39
V_6	0.28	0.16	0.29
CF₃ rotor			
V_3	5.71	5.91	4.74

levels. Under the denotation B3LYP, Gaussian uses the B3 exchange function of Becke [26], while as correlation functional a combination of the Lee-Yang-Parr (LYP) and the Vosko-Wilk-Nusair (VWN) [27] functionals is used. The structural parameters of the *cis* ($\phi = 0°$), the *gauche* ($\phi = 120°$) and the *trans* ($\phi = 180°$) conformers of the molecules (see Figure 1) were optimized by minimizing the energy with respect to all the geometrical parameters. The calculated structural parameters are compared to the corresponding values obtained from experimental data for propanal [28] as given in Table 1. The conformational stabilities were determined by comparing the calculated total energies (Table 2).

Potential functions

CHO asymmetric torsional potential function

The potential surface scan for the CHO internal rotation about the C-C single bond was obtained by allowing the OCCC dihedral angles (ϕ) to vary from $0°$ (*cis* position) to $180°$ (*trans* position). Full geometry optimizations at each of the fixed dihedral angle (ϕ) of, $15°$, $30°$, $45°$, $60°$, $75°$, $90°$, $105°$, $120°$, $135°$, $150°$, and $165°$ were carried out at both levels of calculations. The barrier to interconversion in the molecule was calculated and listed in Table 2. The torsional potential was represented as a Fourier cosine series in the dihedral angle (ϕ): $V(\phi) = \sum(V_n/2)[1-\cos(n\phi)]$, where the potential coefficients from V_1 to V_6 are considered adequate to describe the potential function. The results of the energy optimizations were used to calculate the six coefficients by least-squares fitting (Table 3). The potential function of the CHO group is shown in Figure 2.
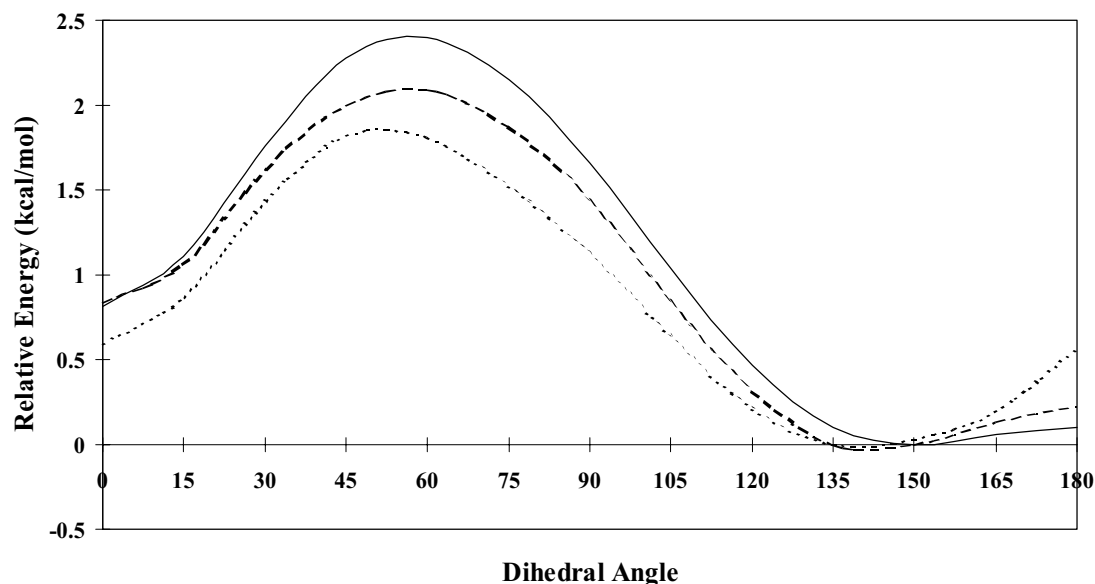
Figure 1 *Atom numbering of 3,3,3-trifluoropropanal in the* cis *conformation*

Figure 2 *Potential function for the asymmetric CHO torsion in 3,3,3-trifluoropropanal as determined by* ab initio *calculations with HF/6-31G** (solid lines), B3LYP/6-31G** (dashed lines), and MP2/6-31G** (dotted lines) respectively*
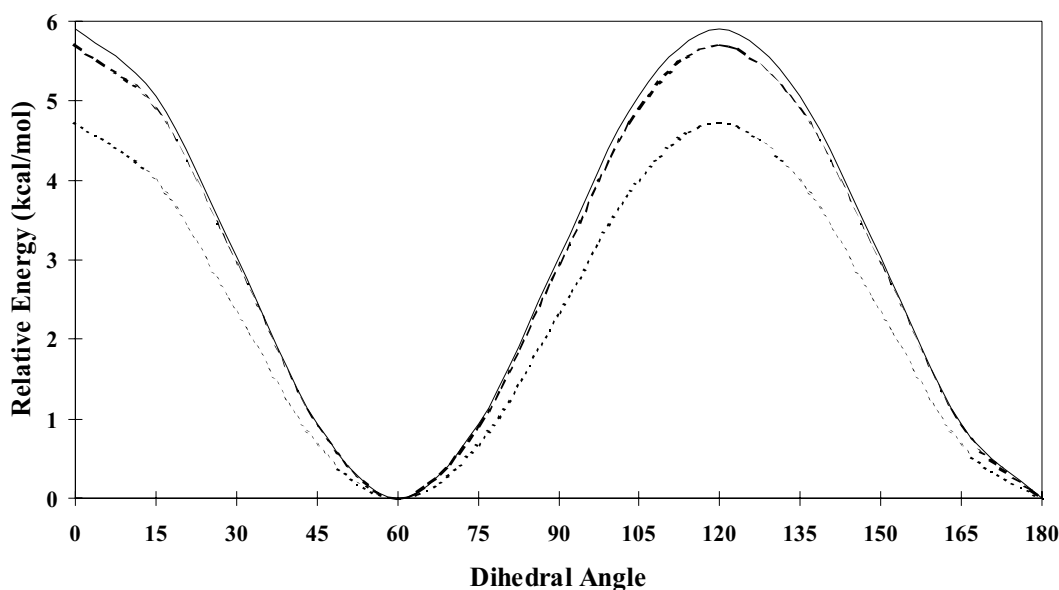

Figure 3 *Potential function for the symmetric CF$_3$ torsion in 3,3,3-trifluoropropanal as determined by* ab initio *calculations with HF/6-31G** (dashed lines), B3LYP/6- 31G** (dotted lines) and MP2/6-31G** (dashed lines) respectively*

CF$_3$ symmetric torsional potential function

The potential function for the CF$_3$ internal rotation about the C-C single bond was obtained by varying the FCCC dihedral angle and repeating the above procedure every 15°. The three-fold potential coefficient of the symmetric CF$_3$ function was listed in Table 3. The CF$_3$ potential scan is shown in Figure 3.

Vibrational frequencies and normal coordinate analyses

The vibrational frequencies for the *cis* ($\phi = 0°$), and the *gauche* ($\phi \cong 120°$) conformers of 3,3,3-trifluoropanal were computed at three levels of calculations. The molecule in the *cis* and *trans* conformers have C$_s$ symmetry. The 24 vibrational modes span the irreducible representations: 15 A' and 9 A''. The A' modes should be polarized while the A'' modes be depolar-

Table 4 *Internal coordinate definitions [a] for 3,3,3-trifluoro-propanal*

No.	Coordinate		Definition
1	C_1-C_2	stretch	R_1
2	C_1-C_3	stretch	R_2
3	C_3-O_4	stretch	S
4	C_3-H_5	stretch	P
5	C_2-F_6	stretch	Q_1
6	C_2-F_7	stretch	Q_2
7	C_2-F_8	stretch	Q_3
8	C_1-H_9	stretch	A_1
9	C_1-H_{10}	stretch	A_2
10	$C_2C_1C_3$	bend	ε
11	$C_1C_3O_4$	bend	θ
12	$C_1C_3H_5$	bend	ϕ
13	$H_5C_3O_4$	bend	ω
14	$C_2C_1H_9$	bend	σ_1
15	$C_2C_1H_{10}$	bend	σ_2
16	$C_3C_1H_9$	bend	γ_1
17	$C_3C_1H_{10}$	bend	γ_2
18	$H_9C_1H_{10}$	bend	ϕ
19	$C_1C_2F_6$	bend	α_1
20	$C_1C_2F_7$	bend	α_2
21	$C_1C_2F_8$	bend	α_3
22	$F_6C_2F_7$	bend	β_1
23	$F_6C_2F_8$	bend	β_2
24	$F_7C_2F_8$	bend	β_3
25	$C_2C_1C_3O_4$ $C_2C_1C_3H_5$	(CFO) torsion	τ_1
26	$F_6C_2C_1C_3$ $F_7C_2C_1C_3$ $F_8C_2C_1C_3$	(CF$_3$) torsion	τ_2
27	$H_5C_3C_1O_4$	wag	η

[a] For atom denotation see Figure 1

ized in the Raman spectrum of the liquid. The *gauche* conformer of the molecule has C_1 symmetry with all the vibrational modes belonging to the A' representation and are polarized in the Raman spectrum of the liquid. The zero-energy corrections were included into the calculated CHO barrier as shown in Table 2.

Normal coordinate analyses were carried out for the stable *cis* and *gauche* conformers to provide a complete assignment of the fundamental vibrational wavenumbers. A computer program was written for this purpose following Wilson's method [29]. The Cartesian coordinates for the stable conformers together with the normal modes (in Cartesian coordinates) and the frequencies from the Gaussian 94 output were used as input in the program. A complete set of internal coordinates was used to form symmetry coordinates (Tables 4 and 5). The normal modes were transformed to mass-weighted Cartesian coordinates, which were then used to calculate the force constant matrix. This was diagonalized

and its eigenvectors and eigenvalues were used in the further calculations. In the output of Gaussian 94 the normal modes are given to an accuracy of only two digits after the decimal points. Therefore, the frequencies obtained in this way are expected to differ from those obtained from the SCF calculation by at most 1 cm^{-1} with the larger differences at higher wavenumbers (less than 1% error). Following this step the force constant matrix was transformed to internal coordinates. To ensure correctness, this transformation was checked numerically in both directions.

At this point the force constant matrix in internal coordinates is calculated and could be scaled if desired, back-transformed to mass-weighted Cartesians and diagonalized again to get scaled frequencies and normal modes. Considering the size of the basis set used and the methods applied (MP2 and DFT) we left the corresponding wavenumbers unscaled. For the purpose of comparison in the case of RHF we list both scaled and unscaled wavenumbers in Tables 6 and 7. The matrix was finally transformed to symmetry coordinates where again all possible numerical checks were performed.

In the next step the normal modes were also transformed to symmetry coordinates. Finally, the potential energy distribution (PED) for each normal mode among the symmetry coordinates was calculated and given in Tables 6 and 7. A tentative assignment of the fundamentals was proposed. The assignments were made based on the calculated PED, infrared band intensities, Raman line activities and depolarization ratios and on those reported for propanal [28] and trifluoro-acetaldehyde [30]. The data of the vibrational assignments are listed in Tables 6 and 7.

Calculation of vibrational spectra

To calculate the Raman spectra we used the frequencies ν_j as calculated at the RHF, MP2 and DFT-B3LYP levels (6-31G** basis set for all), while the scattering activities S_j, and the depolarization ratio ρ_j are available only at RHF, but not at the other two levels. Then the Raman cross-sections ($\partial\sigma_j/\partial\Omega$), which are proportional to the intensities [31,32], are given as:

$$\frac{\partial\sigma_j}{\partial\Omega} = \left(\frac{2^4\pi^4}{45}\right)(\nu_0 - \nu_j)^4 \left(\frac{h}{8\pi^2 c\nu_j}\right) S_j \cdot$$
$$\cdot\left[\left(\frac{1-\rho_j}{1+\rho_j}\right)\right] \Big/ \left[1 - \exp\left(\frac{-hc\nu_j}{k_B T}\right)\right] \qquad (1)$$

Since we use only relative intensities, we calculated them as:

$$I_j = \left(\frac{\partial\sigma_j}{\partial\Omega}\right) \Big/ \left(\frac{\partial\sigma_{jm}}{\partial\Omega}\right) \qquad (2)$$

where *jm* denotes the normal mode having the largest Raman cross-section. As laser wavelength we took $\lambda_0 = 514.5$ nm

Table 5 *Symmetry coordinates for 3,3,3-trifluoropropanal*

Species	Description	Symmetry coordinate [a]
A′		
CH_2	symmetric stretch	$S_1 = A_1 + A_2$
$C-H_{ald}$	stretch	$S_2 = P$
$C=O$	stretch	$S_3 = S$
CH_2	wag	$S_4 = \sigma_1 + \sigma_2 - \gamma_1 - \gamma_2$
CH_2	deformation (scissor)	$S_5 = [(6)^{1/2}+2]\delta - [(6)^{1/2}-2]\varepsilon - \sigma_1 - \sigma_2 - \gamma_1 - \gamma_2$
CH_{ald}	in-plane bend	$S_6 = \phi - \omega$
CF_3	symmetric stretch	$S_7 = Q_1 + Q_2 + Q_3$
CF_3	antisymmetric stretch	$S_8 = 2Q_1 - Q_2 - Q_3$
CCC	antisymmetric stretch	$S_9 = R_1 - R_2$
CCC	symmetric stretch	$S_{10} = R_1 + R_2$
CCO	in-plane bend	$S_{11} = \phi + \omega - 2\theta$
CF_3	symmetric deformation	$S_{12} = \beta_1 + \beta_2 + \beta_3 - \alpha_1 - \alpha_2 - \alpha_3$
CF_3	antisymmetric deformation	$S_{13} = \beta_1 + \beta_2 - 2\beta_3$
CF_3	rock	$S_{14} = 2\alpha_1 - \alpha_2 - \alpha_3$
CCC	bend	$S_{15} = [(6)^{1/2}-2]\delta - [(6)^{1/2}+2]\varepsilon + \sigma_1 + \sigma_2 + \gamma_1 + \gamma_2$
A″		
CH_2	antisymmetric stretch	$S_{16} = A_1 - A_2$
CF_3	antisymmetric stretch	$S_{17} = Q_2 - Q_3$
CH_2	twist	$S_{18} = \sigma_1 - \sigma_2 - \gamma_1 + \gamma_2$
CHO	out-of-plane bend	$S_{19} = \eta$
CH_2	rock	$S_{20} = \sigma_1 - \sigma_2 + \gamma_1 - \gamma_2$
CF_3	antisymmetric deformation	$S_{21} = \beta_1 - \beta_2$
CF_3	rock	$S_{22} = \alpha_2 - \alpha_3$
CF_3	torsion	$S_{23} = \tau_2$
CHO	torsion	$S_{24} = \tau_1$

[a] Not normalized

($\nu_0 = 1/\lambda_0$), which corresponds to an argon ion laser. We assumed the temperature to be $T = 300\ K$.

Then the line shapes are calculated as Lorentzians (L) with a width of $\Delta\nu = 2.5\ cm^{-1}$. Thus, the final spectrum is calculated as:

$$I(\nu) = \sum_j I_j L(\nu - \nu_j) \tag{3}$$

$$L(\nu - \nu_j) = \left(\frac{1}{\pi}\right)\left(\frac{\Delta\nu}{2}\right)\Bigg/ \left[(\nu - \nu_j)^2 + \left(\frac{\Delta\nu}{2}\right)^2\right] \tag{4}$$

$$\int_{-\infty}^{+\infty} L(\nu)d\nu = 1 \tag{5}$$

where *j* runs over all normal modes. For the plots we used a grid of a step size of $10\ cm^{-1}$, but not when a spectral line appears between two consecutive grid points. In this case we inserted 12 points with step size of $0.5\ cm^{-1}$ into this interval, which includes the exact location of the center of the line.
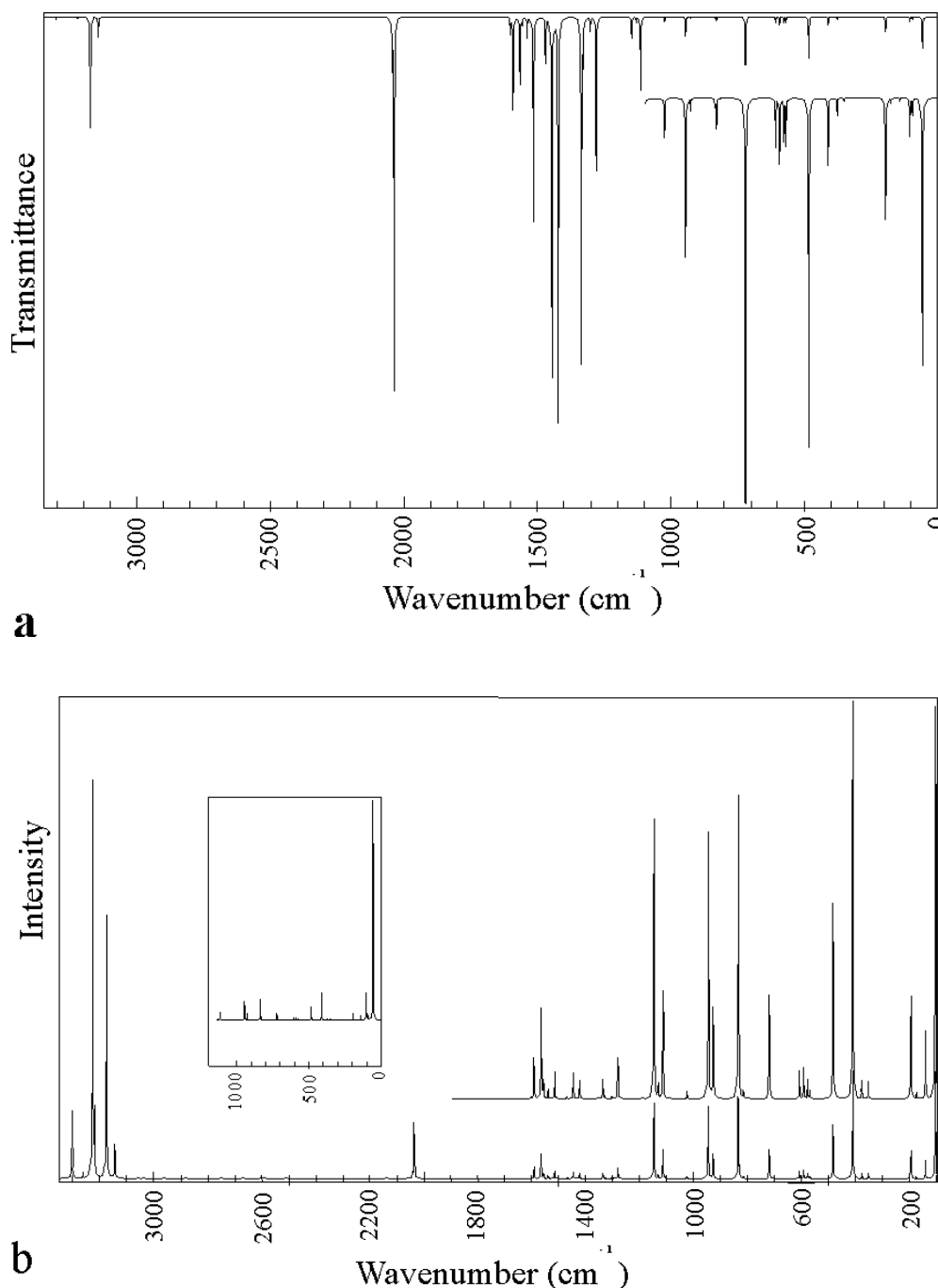
For the infrared spectrum, we used the intensities as given by the respective calculations as they are available on all three levels (relative to the largest one) and converted them to relative transmittance.

The Boltzmann Distribution was then used to superimpose the spectra of the *cis* and the *gauche* conformers of the molecule. Accordingly, the total line intensity was calculated as a function of frequencies. For $N + 1$ different energy minima we have:

$$I(\nu) = \sum_{l=0}^{N} g_l I_l(\nu) e^{-\Delta E_l/k_B T} \Bigg/ \sum_{l=0}^{N} g_l e^{-\Delta E_l/k_B T} \tag{6}$$

where $I_l(\nu)$ are the line intensities for the respective minima, $\Delta E_l = E_l - E_0$, and g_l is a degeneracy factor. Additionally, E_l represents the total energy of conformer *l* corrected with the corresponding zero-point energy. The label *l = 0* is given to the lowest energy conformer. For the temperature, $T = 300\ K$ was used as before. A factor $g_0 = 2$ was used in the calculations to account for the degeneracy of the *gauche* conformer. The calculated vibrational Raman and infrared spectra of the mixture of the two conformers are shown in Figures 4, 5 and 6. The mixture at *300 K* contains 89% *gauche* and 11% *cis* conformer as indicated in the figures. The upper curves in the spectra show an enhanced part of the respective spectrum. The insets in the Raman spectra show the wavenumber region between 0 and 100 cm^{-1} in connection with a part of the rest of the spectra. The 0-100 cm^{-1} part is omitted in the main Raman spectra, because in this

Figure 4 *Calculated vibrational spectra of the mixture of the* cis *and* gauche *conformers of 3,3,3-trifluoropropanal at the RHF/6-31G** level (temperature* T=300K*: 89 %* gauche *and 11 %* cis*).* (**a**) *Infrared spectrum (relative transmittance versus wavenumber).* (**b**) *Raman spectrum (relative intensity versus wavenumber).*

a

b

region the modes assigned to the internal torsions appear with very large intensities. Their inclusion would make the other features of the spectra difficult to see. Figure 4 shows the infrared (a) and the Raman (b) spectrum obtained with RHF, while for the purpose of comparison, Figures 5 and 6 show the spectra obtained with MP2 and DFT/B3LYP respectively. From these figures it is obvious that in RHF spectra all wavenumbers are much higher than in the MP2 and DFT/B3LYP spectra, as expected. The general features of the spectra are actually similar for all three methods, but in RHF at

considerably too high frequencies. Actually, that is the reason why scaling works for RHF, MP2 and DFT do not differ too much in the region of wavenumbers below 2000 cm^{-1}. Most DFT lines are slightly below the respective MP2 lines. However, a few appear also to be shifted slightly upward by DFT. It is clear from the spectra (and also from Tables 6 and 7) that MP2 does not shift the CH stretches downwards from their RHF values appreciably, but DFT does. Therefore, we conclude that in general DFT produces slightly better spectra as compared to experiment than MP2, with much less

Table 6 *Calculated vibrational frequencies (cm^{-1}) at HF/6-31G**, MP2/6-31G** and B3LYP/6-31G** level for the cis conformer of 3,3,3-trifluoropropanal*

No.			HF			MP2		B3LYP		Obs [b]	PED [c]
	Freq.	Scaled [a]	IR Int.	Raman Act.	Depol. Ratio	Freq.	IR Int.	Freq.	IR Int.		
A′											
ν_1	3218	2896	4.2	100.5	0.1	3149	0.8	3062	1.4	2914	100% S_1
ν_2	3145	2831	93.2	107.1	0.4	3029	103.3	2908	114.6	2818	100% S_2
ν_3	2043	1839	209.6	10.1	0.5	1795	92.4	1847	146.5	1754	91% S_3
ν_4	1600	1440	74.5	1.8	0.7	1509	45.5	1464	27.1	1339	55% S_4, 13% S_5, 11% S_6
ν_5	1556	1400	31.0	13.3	0.7	1468	21.8	1433	4.4	1423	57% S_5, 34% S_4
ν_6	1538	1384	96.7	3.0	0.4	1432	124.2	1392	144.2	1381	45% S_6, 21% S_9, 10% S_5
ν_7	1424	1282	199.2	1.6	0.7	1322	151.0	1283	170.4	(1309)	23% S_7, 14% S_8, 17% S_{12}, 14% S_6, 14% S_{10}
ν_8	1329	1196	184.9	2.1	0.7	1219	156.9	1185	155.8	(1193)	56% S_8
ν_9	1024	922	22.0	3.6	0.7	975	25.8	945	29.8	997*	47% S_9, 21% S_4, 11% S_7
ν_{10}	927	834	6.5	6.6	0.1	871	5.0	850	4.1	849	34% S_{10}, 18% S_7, 15% S_{15}, 12% S_{11}
ν_{11}	829	746	17.0	2.4	0.1	766	12.8	758	14.3		22% S_{11}, 34% S_7, 17% S_{12}
ν_{12}	592	533	36.2	2.5	0.4	556	33.2	544	31.7		48% S_{12}, 24% S_{10}, 12% S_{13}
ν_{13}	568	511	26.4	1.7	0.7	522	11.6	517	10.3	(530)	66% S_{13}, 13% S_{11}
ν_{14}	352	317	1.4	0.9	0.5	326	0.6	320	0.4	(254)	57% S_{14}, 19% S_{11}, 11% S_{13}
ν_{15}	176	158	2.4	0.1	0.5	168	1.5	156	1.8	271	66% S_{15}, 18% S_{14}, 13% S_{11}
A″											
ν_{16}	3262	2936	3.8	59.0	0.8	3207	0.5	3103	1.4	2954	100% S_{16}
ν_{17}	1468	1321	216.0	1.9	0.8	1358	161.9	1325	157.7	(1201)	35% S_{17}, 45% S_{18}
ν_{18}	1302	1172	63.2	1.7	0.8	1197	66.6	1172	69.6	1250	31% S_{18}, 30% S_{19}, 25% S_{17}, 10% S_{20}
ν_{19}	1130	1017	26.1	8.4	0.8	1040	30.5	1016	30.2	1127	37% S_{19}, 25% S_{17}, 18% S_{18}, 20% S_{20}
ν_{20}	815	734	0.1	3.0	0.8	760	0.0	741	0.0	658	44% S_{20}, 27% S_{19}, 10% S_{22}
ν_{21}	577	519	2.5	0.4	0.8	530	1.3	523	0.9	(529)	78% S_{21}
ν_{22}	375	338	1.1	0.1	0.8	352	1.3	343	1.5	(323)	72% S_{22}, 14% S_{20}, 11% S_{21}
ν_{23}	141	127	1.4	2.0	0.8	131	0.2	134	0.5	135	52% S_{23}, 44% S_{24}
ν_{24}	94	85	9.3	1.4	0.8	92	5.9	77	5.5	(66)	57% S_{24}, 40% S_{23}

[a] Scaled frequencies are obtained with factors of 0.9 for all modes. Infrared intensities and Raman activies are calculated in Km·mol^{-1} and Å^4·amu^{-1} respectively.

[b] Observed wavenumbers are obtained from Infrared or Raman spectra of gaseous trifluoroacetaldehyde [26], and

propanal [25] respectively. Observed wave-numbers associated with CF$_3$ group are given in parentheses. Asterisk denotes observed Raman wavenumber of the solid.

[c] PED values are obtained by using calculated frequencies at B3LYP level

computational time and expenses. Thus we decided to use the PED values given by DFT for our assignment.

This conclusion is in line with comparative studies on different molecules published in the literature (see ref. [33] and references therein). Calculations on 32 different molecules using a 6-31G* basis and the BLYP functional in DFT show that, while bond lengths and angles are given slightly better by MP2 than by DFT (compared to experiment), dipole moments, harmonic frequencies and atomization energies are given better by DFT than by MP2 [34]. The mean absolute

errors reported in that study on 32 molecules [34] are 0.020 Å (DFT) and 0.014 Å (MP2) for bond lengths, 2.33° (DFT) and 1.78° (MP2) for bond angles, 0.251 D (DFT) and 0.277 D (MP2) for dipole moments, 73 cm^{-1} (DFT) and 99 cm^{-1} (MP2) for harmonic frequencies, and 5.6 kcal mol^{-1} (DFT) and 22.4 kcal mol^{-1} (MP2) for atomization energies. Note that for that study a 6-31G* basis and DFT/BLYP were applied, while we used the improved 6-31G** and DFT/B3LYP. Furthermore, note that while MP2 frequencies were generally too high, the DFT/BLYP values were mostly too low [34].

Figure 5 *Calculated vibrational spectra of the mixture of the* cis *and* gauche *conformers of 3,3,3-trifluoropropanal at the MP2/6-31G** level (temperature* T=300K: *85%* gauche *and 15%* cis*).*
*(**a**) Infrared spectrum (relative transmittance versus wavenumber).*
*(**b**) Raman spectrum (relative intensity versus wavenumber)*
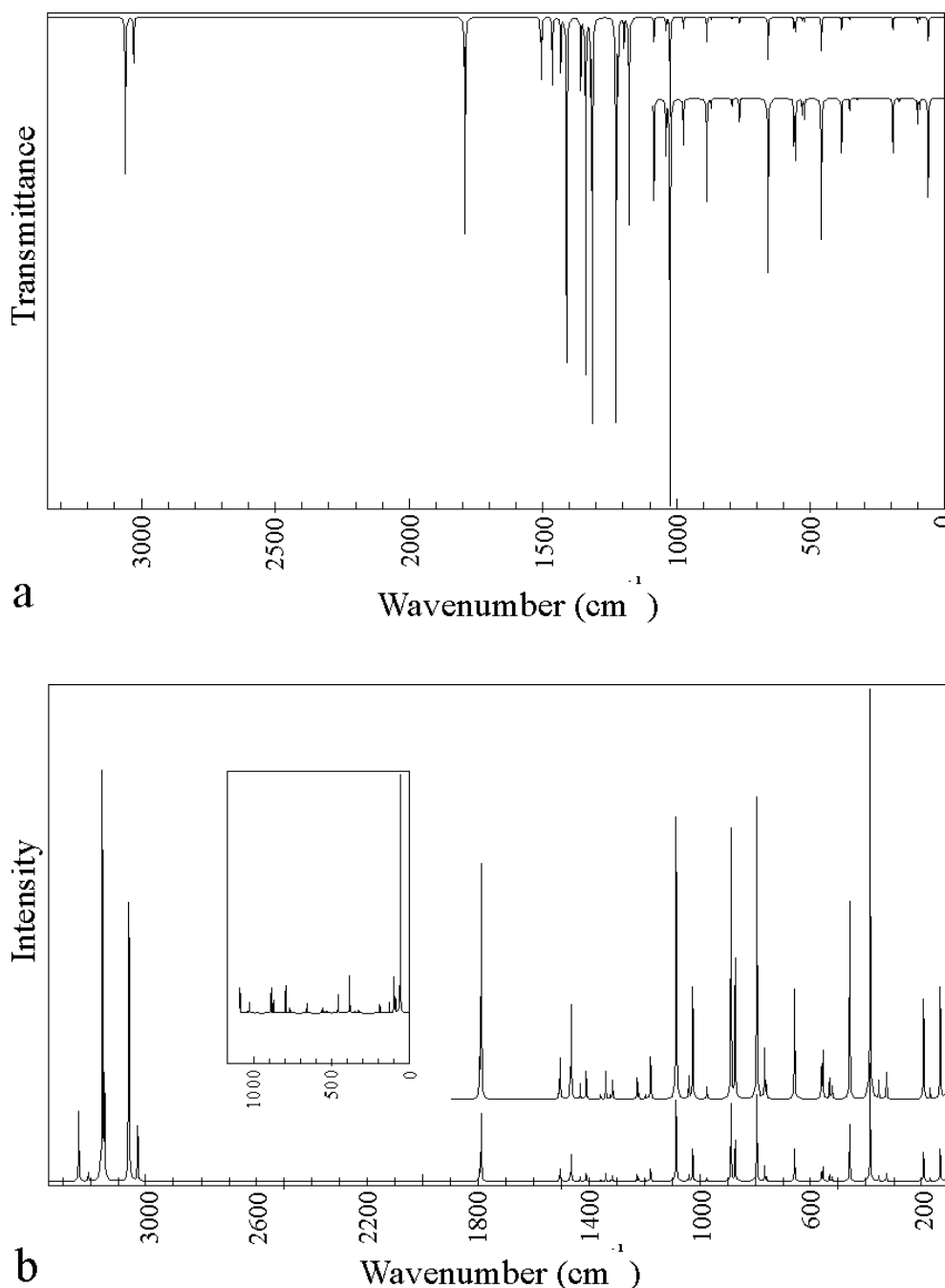
Discussion

The conformational behavior of haloacetaldehydes and halopropanals is generally determined by the strong interaction between the carbonyl oxygen and methylene halogen atoms [7,35,36]. For the corresponding haloacetyl halides [37-39] and halopropionyl halides [16,17] the most stable conformation is the one in which the halogen atoms are away from each other.

In the case of the halopropanes the extent of the interaction depends greatly on how far the carbonyl oxygen is from the halogen atom of the methylene group in the eclipsed position. From the calculations, the equilibrium separation between the oxygen halogen atoms was calculated to be enough for the dipole-dipole interaction to greatly influence the conformational equilibrium. This stabilizes the conformers with minimum oxygen-halogen interaction. This repulsive interaction is also greatly influenced by the size of the halogen atoms. Indeed, 3,3,3-trifluoro- and 3,3,3-trichloropropionyl fluoride and chloride were predicted to have the *cis* form as the thermodynamically preferred conformation [16]. Furthermore, the chloride compound was predicted to exist only in this conformation. The calculated difference in the dipole

Table 7 *Calculated vibrational frequencies (cm^{-1}) at HF/6-31G**, MP2/6-31G** and B3LYP/6-31G** level for the gauche conformer of 3,3,3-trifluoropropanal*

| No. | | HF | | | | MP2 | | B3LYP | | PED[b] |
	Freq.	Scaled [a]	IR Int.	Raman Act.	Depol. Ratio	Freq.	IR Int.	Freq.	IR Int.	
A										
ν_1	3303	2973	1.5	48.8	0.6	3242	0.4	3148	0.9	84% S$_{16}$, 16% S$_1$
ν_2	3226	2903	0.8	87.1	0.1	3156	0.1	3066	0.4	84% S$_1$, 16% S$_{16}$
ν_3	3175	2858	61.9	84.9	0.3	3061	5.1	2943	74.6	100% S$_2$
ν_4	2036	1832	208.8	12.4	0.5	1789	89.6	1842	144.1	92% S$_3$
ν_5	1590	1431	52.1	4.3	0.7	1505	25.4	1461	17.8	90% S$_4$
ν_6	1564	1408	37.6	6.2	0.6	1463	28.2	1435	23.5	80% S$_5$
ν_7	1514	1363	114.9	2.5	0.7	1410	143.5	1362	138.9	39% S$_6$, 18% S$_9$
ν_8	1444	1300	201.4	2.5	0.7	1339	148.0	1306	144.5	41% S$_{18}$, 28% S$_{17}$
ν_9	1421	1279	222.4	1.0	0.6	1315	167.8	1276	174.4	15% S$_7$, 15% S$_8$, 13% S$_6$, 13% S$_{10}$, 13% S$_{12}$
ν_{10}	1335	1202	193.9	1.6	0.7	1226	167.5	1196	181.8	47% S$_8$, 20% S$_6$
ν_{11}	1279	1151	85.9	3.2	0.7	1177	86.4	1153	92.0	30% S$_{18}$, 20% S$_{17}$, 17% S$_{19}$, 13% S$_{20}$
ν_{12}	1146	1031	12.0	5.5	0.3	1085	10.1	1046	13.8	30% S$_9$, 20% S$_{19}$, 20% S$_{20}$, 10% S$_8$, 10% S$_{11}$
ν_{13}	1113	1002	41.0	4.8	0.6	1025	41.0	1004	45.4	32% S$_{17}$, 25% S$_{19}$, 19% S$_{20}$, 16% S$_{18}$
ν_{14}	944	850	10.6	3.3	0.2	887	10.4	868	7.8	43% S$_7$, 31% S$_9$
ν_{15}	835	752	0.5	4.7	0.4	794	0.8	771	0.8	32% S$_{20}$, 22% S$_{19}$
ν_{16}	720	648	27.0	2.4	0.6	657	17.6	648	16.7	50% S$_{12}$, 10% S$_7$
ν_{17}	607	546	3.3	0.5	0.6	561	4.5	553	5.4	51% S$_{13}$, 13% S$_8$, 13% S$_{14}$, 10% S$_{11}$
ν_{18}	576	518	2.6	0.5	0.7	531	1.5	525	1.1	73% S$_{21}$, 10% S$_{17}$
ν_{19}	483	435	23.2	1.5	0.4	459	14.2	449	14.2	47% S$_{11}$, 13% S$_{10}$, 13% S$_{13}$
ν_{20}	411	370	4.5	2.0	0.3	384	5.5	375	5.0	28% S$_{14}$, 21% S$_{10}$, 21% S$_{13}$, 12% S$_{15}$
ν_{21}	376	338	1.2	0.1	0.5	353	1.1	347	1.1	71% S$_{22}$, 12% S$_{21}$
ν_{22}	195	176	8.1	0.5	0.7	192	5.4	186	5.3	53% S$_{15}$, 35% S$_{14}$
ν_{23}	104	94	2.5	0.8	0.7	100	2.5	92	3.0	88% S$_{23}$, 10% S$_{24}$
ν_{24}	57	51	17.8	2.1	0.7	61	9.9	67	9.5	83% S$_{24}$, 11% S$_{23}$

[a] Scaled frequencies are obtained with factors of 0.9 for all modes. IR intensities and Raman activies are calculated in Km·mol^{-1} and Å^4·amu^{-1} respectively.

[b] PED values are obtained by using calculated frequencies at B3LYP level.

moments of the two stable conformers indicated small charge density variations with the rotation of the carbonyl group about the C-C bond [16]. Therefore, it was concluded that dipolar effects were expected to play a less important role than steric forces in the determination of the conformational and structural stability of such molecules [16].

In the present study we have carried out energy optimizations and calculated the vibrational frequencies for the *cis,* the *trans* and the *gauche* conformations of 3,3,3-trifluoropropanal. The calculations were performed with different methods of calculations for comparative purposes. We included electron correlation in the calculations at MP2 level and carried out density functional calculations at B3LYP level. From the calculations, the B3LYP level provided better vibrational frequencies than those obtained at the MP2 level (Tables 6 and 7) with significantly less computation time. We carried out normal coordinate calculations using the vi-

brational wavenumbers obtained at the B3LYP/6-31G** level for both the stable *cis* and *gauche* conformations. We calculated the potential energy distribution PED for each normal mode among the symmetry coordinates for the two conformers of the molecule.

We proposed vibrational assignments for the normal modes of the two stable forms based on the calculated PED values, infrared line intensity, and Raman activities. The assignments of most of the fundamental vibrations were straightforward based on the PED values.

Three of the 24 fundamentals of 3,3,3-trifluoropropanal are C-H stretches, one of which is from the aldehydic group and two are from the methylene group. These three stretches were calculated to have the highest Raman activities for both conformers. For the planar *cis* conformer, the aldehydic C-H and the two CH$_2$ stretches were predicted to have no mixing with each other (Table 6). In the case of the *gauche* con-

Figure 6 *Calculated vibrational spectra of the mixture of the* cis *and* gauche *conformers of 3,3,3-trifluoropropanal at the B3LYP/6-31G** level (temperature* T=300K*: 89%* gauche *and 11%* cis*).*
(**a**) *Infrared spectrum (relative transmittance versus wavenumber).*
(**b**) *Raman spectrum (relative intensity versus wavenumber)*
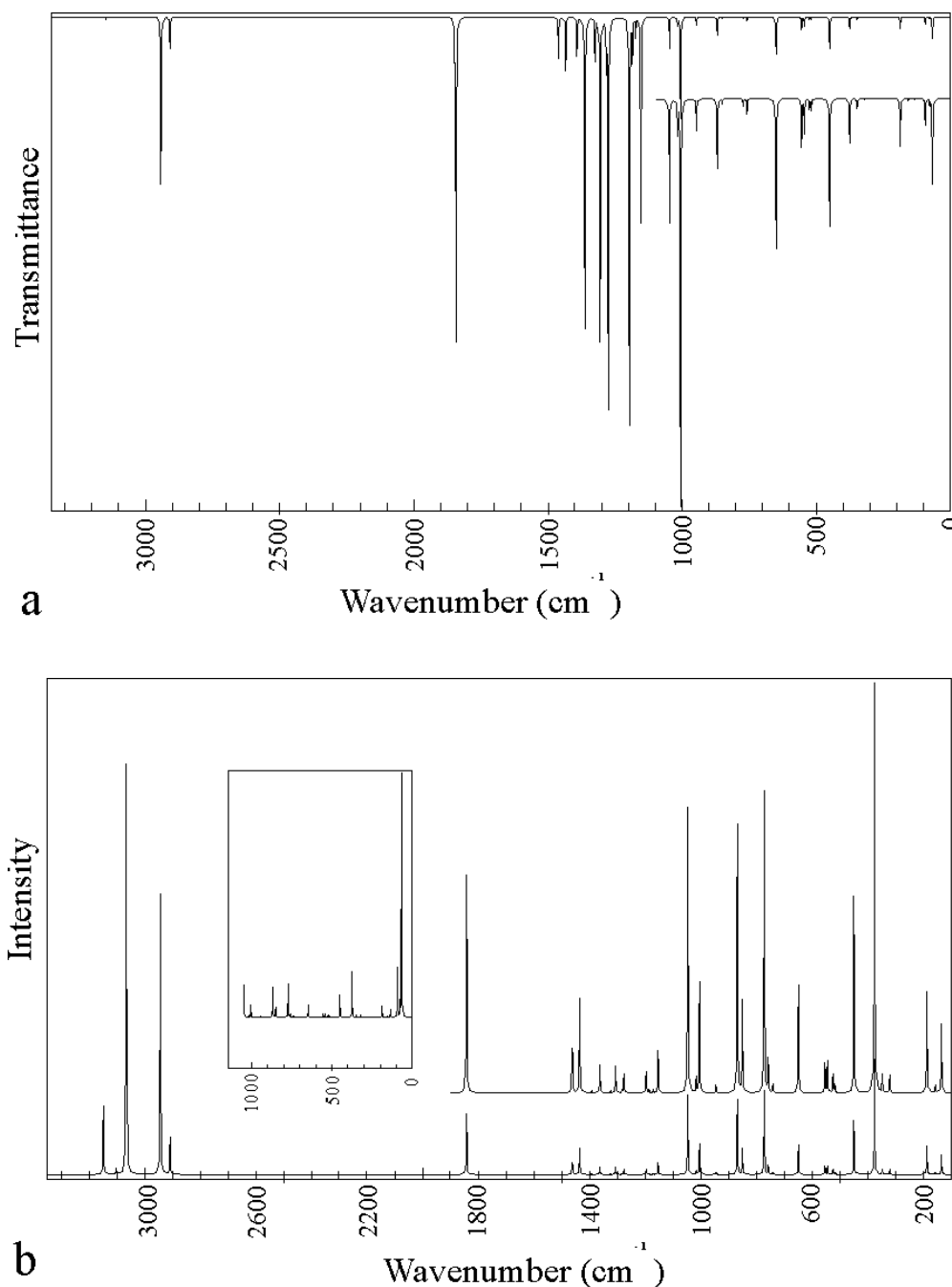
former, the symmetric and asymmetric CH_2 stretches were calculated to mix slightly with each other as shown in Table 7. The aldehydic C-H stretch were calculated to be the lowest of the three at 2908 cm^{-1} (B3LYP). As for the carbonhydrogen bending modes, all were calculated to be mixed with other vibrations. The A' CH_2 scissoring and wagging modes were predicted to be higher in frequeny than the A'' CH_2 twisting mode.

The calculated frequencies at 1847 and 1842 cm^{-1} (B3LYP) in the spectra of the two conformers with very high infrared line intensity are easily assigned to the carbonyl C=O stretch.

This mode was calculated to have a small amount of mixing for the *cis* (91% PED) and the *gauche* (92% PED) conformer. The CCO in-plane bend was observed at 661 cm^{-1} in the infrared spectrum of gaseous propanal [28]. This mode (S_{11}) is calculated at 758 cm^{-1} (B3LYP) with a PED value of 22% in the spectrum of 3,3,3-trifluoroprpanal.

The assignment of the two CCC stretches were clearly to ν_9 (47% S_9) and ν_{10} (34% S_{10}) in the spectrum of the *cis* 3,3,3-trifluoropropanal (Table 6). The calculated wavenumbers of these vibrational modes at B3LYP level are in reasonable agreement with those observed for propanal as shown in Table 6.

The calculated wavenumbers with the highest IR intensities in the spectra of the *cis* and *gauche* conformers could be assigned with confidence to the three C-F stretches. However, these vibrations (ν_7, ν_8, and ν_{17} in the spectrum of the *cis* form) are predicted to be highly mixed with neighboring vibrations. This was not the case for the bending modes associated with the CF_3 moiety, in which a lower degree of mixing was predicted. Therefore, their assignment is straightforward, particularly for the *gauche* conformer, as shown in Tables 6 and 7.

The predicted bending modes that are associated with the CF_3 moiety in the spectrum of 3,3,3-trifluoropropanal are noticed to be rather off those observed in the infrared or Raman spectra of trifluoroacetaldehyde [29]. For example, the CF_3 symmetric deformation is observed at 707 cm^{-1} in the Raman spectrum of gaseous trifluoroacetaldehyde, but is calculated at 544 cm^{-1} (B3LYP) in the spectrum of 3,3,3-trifluoropropanal (Table 6). This could be easily assigned to the in-plane Bending of the CCO group (ν_{11} in the spectrum of the *cis* form with 22% S_{11}). However, the 544 cm^{-1} frequency is predicted to have a PED value of 48% S_{12}, which is obviously the CF_3 symmetric deformation.

Similarly, the CCC bend is observed at 271 cm^{-1} in the infrared spectrum of propanal, while is calculated at 156 cm^{-1} in the spectrum of 3,3,3-trifluoropropanal (66% S_{15}) as given in Table 6. This discrepancy can be explained by understanding the nature of forces that control the structural stability of both trifluoroacetaldehyde and 3,3,3-trifluoropropanal. The presence of a CH_2 group in the middle between the carbonyl and the CF_3 groups reduced significantly the coupling between these two polar groups in 3,3,3-trifluoropropanal as compared to that in trifluoroacetaldehyde.

The lowest vibrations in the spectrum of 3,3,3-trifluoropropanal are the asymmetric CHO and the symmetric CF_3 torsions. These two modes are predicted to mix with each other and are assigned with confidence to ν_{23} and ν_{24}.

In conclusion, we were able to provide reliable vibrational assignments for the normal modes of the two stable conformers of 3,3,3-trifluoropropanal based on normal coordinate calculations. The proposed vibrational assignments were shown to be in very reasonable agreement with those made for similar molecules. Only some discrepancy was noticed in the assignments of several of the modes. This discrepancy was explained as a result of the coupling between these vibrations specially the bending modes that are associated with the heavy atoms of the molecule.

References

1. Guirgis, G. A.; Little, T. S.; Badawi, H. M.; Durig, J. R. *J. Mol. Struct.* **1986,** *142,* 93.
2. Badawi, H. M. *J. Mol. Struct. (Theochem)* **1990,** *208,* 7.
3. Badawi, H. M. *J. Mol. Struct. (Theochem)* **1990,** *208,* 271.
4. Badawi, H. M. *J. Mol. Struct. (Theochem)* **1991,** *228,* 159.
6. Badawi, H. M. *J. Mol. Struct. (Theochem)* **1992,** *276,* 251.
7. Badawi, H. M. *J. Mol. Struct. (Theochem)* **1994,** *314,* 301.
8. Badawi, H. M. *J. Mol. Struct. (Theochem)* **1994,** *336,* 21.
9. Badawi, H. M. *J. Mol. Struct. (Theochem)* **1995,** *343,* 117.
10. Badawi, H. M.; Al-Rayyes, A. A. *J. Mol. Struct. (Theochem)* **1997,** *397,* 51.
11. Badawi, H. M.; Al-Rayyes, A. A. *J. Mol. Struct. (Theochem)* **1998,** *428,* 247.
12. Badawi, H. M.; Förner, W.; Al-Rayyes, A. A. *J. Mol. Model.* **1998,** *4,* 158.
13. Förner, W.; Badawi, H. M. *Asian J. Spectrosc.* **1998,** *2,* 72.
14. Badawi, H. M.; Förner, W. *Asian J. Spectrosc.* **1998,** *2,* 113.
15. Badawi, H. M.; Förner, W. *J. Raman Spectrosc.* **1998,** *29,* 1009.
16. Badawi, H. M.; Förner, W. *J. Mol. Struct. (Theochem)* **1998,** *452,* 85.
17. Badawi, H. M.; Förner, W. *J. Mol. Struct. (Theochem)* **1999,** *488,* 69.
18. Bell, S.; Bisset, A.; Dines, T. J. *J. Raman Spectrosc.* **1998,** *29,* 447.
19. Durig, J. R.; Xiao, A.; Robb, J. B. II; Daeyaert, F. F. D. *J. Raman Spectrosc.* **1998,** *29,* 463.
20. Stratmann, R. E.; Scuseria, G. E.; Frisch, M. J. *J. Raman Spectrosc.* **1998,** *29,* 483.
21. Hudson, B. S.; Markham, L. M. *J. Raman Spectrosc.* **1998,** *29,* 489.
22. Negri, F.; Orlandi, G. *J. Raman Spectrosc.* **1998,** *29,* 501.
23. Vazquez, J.; Lopez Gozales, J. J.; Marquez, F.; Boggs, J. E. *J. Raman Spectrosc.* **1998,** *29,* 547.
24. Gaussian 94, Frisch, M. J.; Trucks, G. W.; Schlegel, H. B.; Gill, P. M. W.; Johnson, B. G.; Robb, M. A.; Cheeseman, J. R.; Keith, T.; Petersson, G. A.; Montgomery, J. A.; Raghavachari, K.; Al-Laham, M. A.; Zakrzewski, V. G.; Ortiz, J. V.; Foresman, J. B.; Cioslowski, J.; Stefanov, B. B.; Nanyakkara, A.; Challacombe, M.; Peng, C. Y.; Ayala, P. Y.; Chen, W.; Wong, M. W.; Andres, J. L.; Replogle, E. S.; Gomperts, R.; Martin, R. L.; Fox, D. T.; Binkley, J. S.; Defrees, D. J.; Baker, J.; Stewart, J. J. P.; Head-Gordon, M.; Gonzalez, C.; Pople, J. A.; Gaussian, Inc.: Pittsburg PA, 1995.
25. Møller, C.; Plesset, M. S. *Phys. Rev.* **1934,** *46,* 618.
26. Becke, A. D. *J. Chem. Phys.* **1993,** *98,* 5648.
27. a) Lee, C.; Yang, W.; Parr, R. G. *Phys.Rev.* **1988,** *B37,* 385; b) Vosko, S. H.; Wilk, L.; Nusair, M. *Can J. Phys.* **1980,** *58,* 1200.
28. Guirgis, G. A.; Drew, B. R.; Gounev, T. K.; Durig, J. R. *Spectrochim. Acta* **1998,** *54A,* 123.
29. Wilson, E. B.; Decius, J. C.; Cross, P. C. *Molecular vibrations* McGraw-Hill: New York, 1955.
30. Durig, J. R.; Guigis, G. A.; van der Veken, J. B. *J. Raman Spectrosc.* **1987,** *18,* 549.
31. Durig, J. R.; Guirgis, G. A.; Krutules, K. A.; Phan, H. V.; Stidham, H. D. *J. Raman Spectrosc.* **1994,** *25,* 221.

32. Chantry, G. W. In The Raman Effect; Anderson, A., Ed.; Marcel Dekker: New York, 1971**;** Vol. 1, Chapter 2.

33. Handy, N. C. In Lecture Notes in Quantum Chemistry II; Roos, B. O., Ed.; Springer-Verlag: Berlin, Heidelberg, 1994; pp. 91-124.

34. Johnson, B.; Gill, P. M. W.; Pople, J. A. *J. Chem. Phys.* **1993**, *98*, 5612.

35. Durig, J. R.; Phan, H. V.; Little, T. S. *J. Mol. Struct. (Theochem)* **1989**, *202*, 143.

36. Phan, H. V.; Durig, J. R. *J. Mol. Struct. (Theochem)* **1989**, *202*, 333.

37. Little, T. S.; Wang, A. Y.; Durig, J. R. *J. Mol. Struct.* **1990**, *217*, 221.

38. Durig, J. R.; Wang, A. Y.; Little, T. S. *Int. Rev. Phys. Chem.* **1990**, *9*, 349.

39. Durig, J. R.; Bergana, M. M.; Phan, H. V. *J. Mol. Struct.* **1991**, *242*, 179.